Frequency Identification of Bridges Using Smartphones on Vehicles with Variable Features

Article *in* Journal of Bridge Engineering · December 2019

DOI: 10.1061/(ASCE)BE.1943-5592.0001565

Frequency Identification of Bridges using Smartphones on Vehicles with Variable Features

Nima Shirzad-Ghaleroudkhani
Graduate Student, shirzadg@ualberta.ca, Dept. of Civil and Environmental Engineering, University of Alberta, Edmonton, Alberta, T6G 1H9, Canada

Qipei Mei
Graduate Student, qipei@ualberta.ca, Dept. of Civil and Environmental Engineering, University of Alberta, Edmonton, Alberta, T6G 1H9, Canada

Mustafa Gül
Associate Professor, mustafa.gul@ ualberta.ca, Dept. of Civil and Environmental Engineering, University of Alberta, Edmonton, Alberta, T6G 1H9, Canada

Abstract

This paper puts forward a crowdsensing framework for employing smartphones in monitoring populations of bridges in future smart cities. In this regard, since there are a variety of vehicles with different features traveling over the bridge at different speeds, it is critical to investigate the robustness of indirect monitoring methods against vehicle features. Hence, an experimental study has been performed, including two lab-scale bridges with different boundary conditions and a robot car capable of maintaining a variety of speeds and suspension systems. The proposed framework focuses on the identification of frequencies of the bridge using acceleration signals recorded on the car. It is demonstrated that through a large set of passing cars with different features, the fundamental frequency of the bridge can be captured. Successful identification of the deviation of fundamental frequencies between two bridges with relatively close frequency values proves that the framework is capable of detecting damage-induced frequency changes of the bridge. Since this framework relies on using smartphones, it provides the opportunity to efficiently monitor a plethora of bridges in a metropolitan with minimum cost.

Keywords: Smart city; Indirect monitoring; Bridge; Smartphone; Frequency analysis.

Introduction

Urban population growth in recent decades has created complications in the management of urban cities (Graham 2010). To overcome such difficulties, the concept of Smart City has been developed by employing smart sensing, computing, and communication technologies in urban management (Chourabi et al. 2012; Washburn et al. 2010). Applications of smart technologies in transportation infrastructure have been widely studied in the literature (Adeli and Jiang 2009; Glancy 2014; Xiong et al. 2012). Bridges, as key components of transportation networks, are prone to structural damage resulting in an irrecoverable financial and time loss (Ham et al. 2005). Many bridge structures in modern countries have reached their design life and will need to be monitored and retrofitted to remain in service in a cost-effective manner. For example, according to Canadian Infrastructural Report Card (2016), about 26% of bridges in Canada are in fair, poor, or very poor conditions. Sustainability of transportation networks relies on appropriate monitoring and maintenance operations on bridges. Hence, Structural Health Monitoring (SHM) techniques have been proposed as a critical component of viable transportation networks (Wenzel 2008).

Traditionally, most of the proposed SHM methods require bridge instrumentation with fixed sensors installed on the bridge; see Catbas et al. (2008), Guan et al. (2018), Gul and Catbas (2009), Hoult et al. (2010), Hsieh et al. (2006), Ko and Ni (2005), and Wong (2004) among others. The functionality and accuracy of these methods have been demonstrated in those studies. However, the feasibility of employing such direct SHM methods to a large number of bridges is a major concern. Instrumentation of each bridge with fixed sensors and creating a data collection network is costly and time-consuming, and cannot be employed to all bridges. Hence, new SHM methods have been suggested through focusing on sensors placed in passing vehicles as moving sensors, i.e. indirect monitoring of bridges.

Indirect bridge monitoring concept was first proposed by Yang et al. (2004). They performed a dynamic analysis of vehicle-bridge interaction for a simple 2D beam model representing the bridge and a moving mass-spring system representing the vehicle. It was shown that the frequency of the bridge can be extracted from the vibration of the vehicle. Afterward, many studies followed indirect bridge monitoring (Malekjafarian et al. 2015), which can be divided into analytical/numerical studies (Hattori et al. 2012; Hester and González 2017; Keenahan et al. 2014; OBrien et al. 2017; Yang and Chen 2016), lab-scale experiments (Cerda et al. 2014; Mei et al. 2019; Zhang et al. 2013), and real-life experiments (Kim and Lynch 2012; Lin and Yang 2005; Siringoringo and Fujino 2012). All these studies corroborate the fact that bridge dynamic response exists in the vibration of the passing vehicle and can be extracted to assess the bridge condition. Hence, instrumentation of vehicles with accelerometers may provide an effective source of monitoring many bridges within a city. More recently, an alternative way of employing indirect monitoring methods using the smartphones of the passengers in vehicles has been proposed by several research groups as discussed below.

In the context of smart cities, smartphones are critical devices as they may provide valuable crowdsensing data. They have important sensors, including accelerometer, gyroscope, GPS, etc., which can be used in monitoring of different structures (Feng et al. 2015; Kong et al. 2018; Morgenthal et al. 2018; Ozer and Feng 2016, 2017; Zhao et al. 2017). In regard to transportation network, smartphones have been previously proved as an effective tool to estimate traffic incidents, like congestions or accidents (Bhoraskar et al. 2012; Händel et al. 2014; Mohan et al. 2008). However, their application to indirect SHM had not been investigated until recent studies show that smartphones can be used as reliable sensors to collect acceleration data and apply them into indirect health monitoring techniques to assess bridge conditions. Mei and Gül (2018) proposed an indirect damage detection method based on Mel-frequency cepstral coefficients and used a smartphone to detect multiple damage states on a lab-scale bridge model. They showed for the first time in the literature that the damage in the bridge model can be identified using the smartphone on a car model even if the speed, weight, and suspension of the car are varied between experiments. In another study, Matarazzo et al. (2018) performed a real-life experiment to investigate the possibility of capturing bridge frequencies using smartphones. These studies arrive at the same conclusion that the recorded vibration of the vehicle is highly dominated by vehicle features, such as suspension, mass, speed, etc.

Previously, many experiments studied the effect of car features on the frequency spectrum of the vehicle. Most of the past studies on indirect health monitoring of bridges were conducted using dedicated professional accelerometers placed in the vehicles to collect data from the car while this study focuses on using smartphones as data collecting devices in future smart cities. Li et al. (2019) studied the effect of speed on the frequency content recorded on the cars passing over the bridge through a lab scale test. Their conclusion was that lower speeds benefits the process of frequency identification. Similar conclusion was made in another study by Kim et al. (2011). However, the car models in both studies were not motorized while the data in our experiments shows that the main effect of the change in the speed of the car on the spectrum is due to the change in the revolving speed of the motor, which is also expected in real-life practice. In another study, Mei et al. (2019) conducted laboratory experiments where both speed and suspension stiffness of the car were considered. However, the damage detection method employed in that study did not focus on the modal analysis of the acceleration data.

In regard to large-scale indirect monitoring of populations of bridges in smart cities, where there are different vehicles with different features traveling at different speeds, it is vital to investigate the robustness of indirect monitoring method using smartphones against vehicle features. Hence, this study focuses on the application of smartphones in different cars traveling at different speeds to capture frequencies of the bridge. Several laboratory experiments are conducted using two experimental bridge models with different support conditions, and also a robot car model capable of changing suspension springs and traveling speeds. In total, three spring types and three speeds were applied to the car, resulting in 9 combinations. The experiment consists of three stages. First, vibration analysis of the bridge is conducted to extract natural frequencies of the bridge. Next, robot car vibration is analyzed to study the frequency spectrum of the car while moving on a rigid non-vibrating surface. Finally, the vibration of the car while moving on the bridge is studied. Comparing results of these three stages provides the possibility of investigating the robustness of using smartphones to capture bridge frequencies against vehicle features.

Methodology

In this section, first the fundamental notion of vehicle-bridge interaction and its application to this research is explained. Afterward, the frequency-domain analysis applied to the vibration signals is described.

Vehicle-bridge Interaction

Vehicle-bridge interaction (VBI) is the main concept in indirect bridge monitoring. Due to the dynamic interaction, vibrations of vehicle and bridge are coupled to each other. In other words, the vibration of a vehicle moving over a bridge consists of both the vehicle and the bridge vibration. One of the first studies to investigate this notion was performed by Yang and Yau (1997). In that study, a simple 2D beam model was used to model a bridge and a moving spring-mass system was considered as the vehicle. The following equation was derived in that paper:

$$\begin{cases} \bar{m}(x)u_b^{''}(x,t) + E(x)I(x)u_b^{'''}(x,t) = c(x,t) \\ m_v u_v^{''}(t) + k_v\left[u_v(t) - u_b(x,t)\right] = 0 \end{cases} \tag{1}$$

where x is the distance to the bridge end, t is the time, v is the speed of the vehicle, $\bar{m}(x)$ is the distributed mass of the bridge per unit length, $E(x)$ and $I(x)$ are the elastic modulus and moment of inertia of the bridge section, respectively, m_v and k_v are the mass and stiffness of the vehicle, and $c(x, t)$ is the contact force. Furthermore, u_b and u_v are the vertical displacements of the bridge and the vehicle relative to the equilibrium position, respectively. The first equation is the governing dynamic equilibrium of the bridge, and the second one is of the vehicle. As seen in Eq. (1), the dynamic response of the vehicle includes dynamic characteristics of the bridge which means using an appropriate signal processing technique, it would be possible to extract bridge dynamic features, e.g. frequencies, from the vibration of the vehicle. Although this model is simple and does not account for many challenges such as complicated vehicle model, road roughness, and environmental effects, the fact that the dynamic features of the bridge exist in the vibration of the vehicle still governs.

Frequency-domain analysis

In this research, frequency content of the acceleration signal is calculated through an averaging method proposed by Welch (1967), here called Averaged Discrete Fourier Transform (ADFT), by averaging Fourier Transforms of the main signal over small windows. Eq. (2) describes Discrete Fourier Transform (DFT) as follows:

$$X[k] = \sum_{n=0}^{N-1} u_v''[n] e^{-j\frac{2\pi}{N}kn} \tag{2}$$

In this equation, u_v'' shows the acceleration signal recorded on the vehicle as previously defined in Eq. (1), N is the number of data points in the signal, and X denotes vector of DFTs, which is a complex vector containing amplitude and phase values. Moreover, k is an index representing step frequencies through the following equation:

$$f = \frac{k}{N} f_s \qquad \text{for } 0 \leq k \leq N-1 \tag{3}$$

where f_s is the sampling frequency. Applying Eq. (2) to the whole acceleration signal results in a highly fluctuated spectrum, which is not suitable for peak analysis. However, if the signal is divided into multiple segments and each segment is considered as a separate signal in the DFT process, following by averaging all the spectrums, the resulting spectrum will be smoother and more convenient for peak analysis. Among a variety of window functions proposed for selecting sub-signals (Harris 1978), hamming window is considered in this study. In addition, selected windows are not mutually exclusive to account for the effect of the transition and a percentage of the window length is considered as an overlap. Therefore, the ADFT of the signal is calculated through the following equation:

$$\bar{X}[k] = \frac{1}{M}\sum_{m=1}^{M}\sum_{n=0}^{N-1} w_m[n]u_v''[n]\mathrm{e}^{-j\frac{2\pi}{N}kn} \tag{4}$$

In Eq. (4), w_m is the function for m^{th} window and M is the total number of windows calculated by

$$M = 1 + \frac{N - N_w}{(1-p)\cdot N_w} \tag{5}$$

in which p is the overlap percentage of the windows. In this paper, since the lengths of most acceleration signals are between 6 to 12 seconds, 5 seconds hamming window and 75% overlap are considered. To increase the frequency resolution of ADFT spectrum, all windows are zero-padded to 10 seconds, resulting in a 0.1 Hz resolution. Furthermore, the acceleration signals from the smartphone are resampled by interpolation before being converted to the frequency domain. The reason is that the sampling intervals of smartphones may not be perfectly consistent and deviate from the pre-set value. Although the android application developed in authors' research group (Mei and Gül 2018) significantly improves the stability of sampling frequency, resampling of the signal still increases the accuracy of the calculation.

In order to identify the most significant frequencies in each spectrum, a peak picking technique based on amplitude and prominence has been employed using MATLAB (Mathworks 2018). The prominence of a peak represents how the peak stands out due to its intrinsic height and location with respect to other adjacent peaks. A low but isolated peak can be more prominent than another one that is higher but is among a range of tall peaks. On the other hand, two equally prominent peaks with a substantial difference in the amplitude are not equally significant in a spectrum. Hence, both the prominence and amplitude are considered as the criteria in this study. To this end, the amplitude and prominence values for all peaks in a spectrum are scaled to 100, and the peak score is defined as the average of its amplitude and prominence scores. This averaged score is then used as a criterion to quantify significance of the peaks in the spectrum.

Experimental setup

This section illustrates the material and devices used in this experiment. First, two bridge models are described. Subsequently, the features of the robot-car are explained. Finally, the instruments utilized to collect data during the experiment are presented.

Bridge

In this study, two types of bridges, one pin-roller and one fixed-fixed support, are considered. For both bridges, hot rolled steel plates of W44, which has the modulus of elasticity of 200 GPa, yield strength of 250 MPa, and ultimate strength of 310 MPa, are used. These plates are 2 m long and 330 mm wide. The thickness of the plates in two bridge types are different: a 12.7 mm thick plate is used for the pin-roller bridge setup whereas a 6.35 mm thick plate is used for the fixed-fixed bridge setup. The reason for this selection is that using the low thickness plate for pin-roller support bridge results in a significant sag in the middle of the bridge, which prevents the speed of the robot car to be constant while traveling over the bridge. On the other hand, using a thick plate for the fixed-fixed support bridge will intensively increase the stiffness and frequency of the bridge, which not only makes the bridge vibration negligible with respect to the car, but also makes the experiment unrealistic.

Fig. 1 shows the setup for the pin-roller bridge. Here, one pin support and one roller support are employed to carry the 12.7 mm thick plate. In Fig. 2, the pin-roller support structure is illustrated. Both supports have the same structure, except that the pin is prevented from moving horizontally while the roller is free to move. As seen, an approaching span is also considered for the first few seconds that the car accelerates and reaches the constant target speed. Furthermore, another plate is used at the end of the bridge so that the car completely leaves the bridge and then stops. An additional small thick plate is employed between the main span plate and the supports so that the approaching and end spans do not have any contact with the supports and hence do not affect their free rotation.

Fig. 1. Pin-roller bridge setup

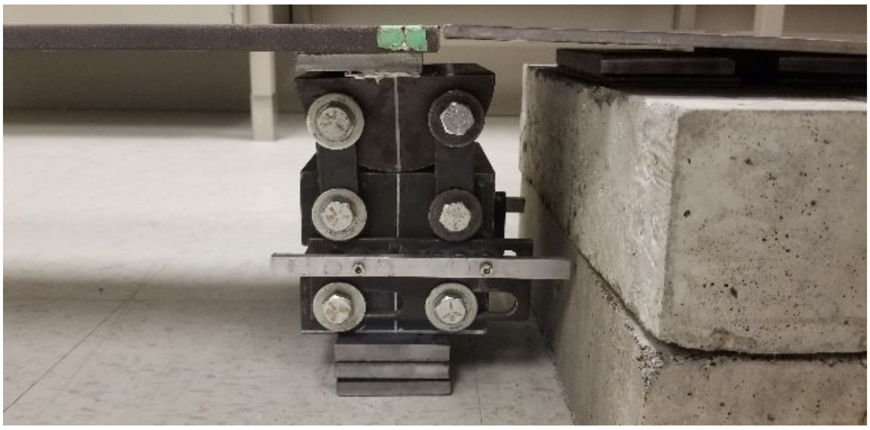

Fig. 2. Pin/roller support

Fig. 3 demonstrates the setup for the fixed-fixed bridge. In this bridge, both supports are assumed to be completely fixed. In order to reach full fixity, two 25 cm long W10×54 steel profile beams are used as the supports, which are connected to the main span plate of 6.35 mm thick through four bolts on both sides, as seen in Fig. 4. In addition, to prevent the supports from moving horizontally, nine reinforced concrete blocks are used at both ends. Similar to the pin-roller bridge, two plates are used as the approaching and end spans.

Fig. 3. Fixed-fixed bridge setup

Fig. 4. Fixed support

Vehicle

In this study, a robot car was designed and built as shown in Fig. 5 and Fig. 6. This car consists of two identical rectangular aluminum plates of 350 mm by 125 mm with the thickness of 3.1 mm. The motor and the wheels are connected to the bottom plate. Four aluminum rods with the radius of 4 mm and length of 15 cm surrounded by four springs are used to connect the bottom plate to the top plate, where the acceleration data will be collected. Four linear bearings are connected to the top plate to ensure a smooth vertical movement on the springs.

The robot car in this experiment is capable of maintaining constant speeds between 0.2 and 0.4 m/s over flat surfaces or gentle slopes. Thus, three speed cases of 0.2, 0.3, and 0.4 m/s are considered here. In addition, in order to model three different suspension systems, three springs with stiffness values of 425, 615 and 726 N/m are employed. These springs are herein referred to as A, B, and C, respectively. The total mass of the top plate, including the smartphone and the sensor, is kept constant to 1.2 kg in all cases to make a better comparison of the effect of the suspension system on the spectrum of the passing car.

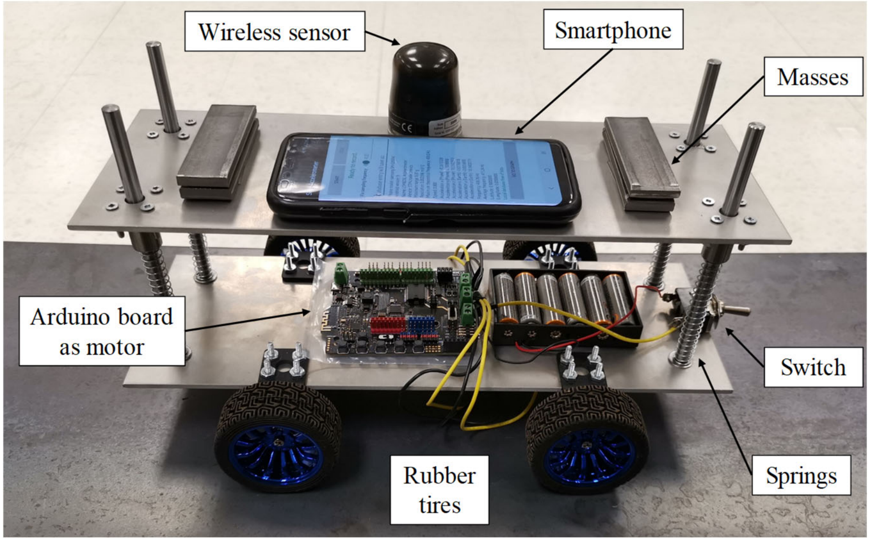

Fig. 5. The custom-designed and -built robot car

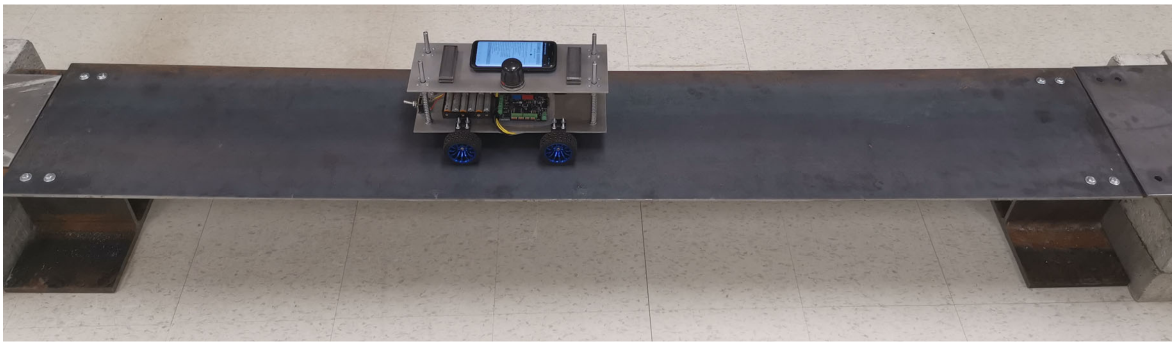
Fig. 6. Robot car on the fixed-fixed bridge

Instrumentation

To collect the acceleration from the car, one smartphone, Samsung Galaxy S8, with the sampling frequency of 400 Hz is used. Recording acceleration data from the smartphone is performed using an android app previously developed and used in (Mei and Gül 2018), which provides the global vertical acceleration by using gyroscope and magnetometer in combination with accelerometer. This app also applies sampling frequency correction to the recorded data. In addition to the smartphone and in order to have a benchmark for comparison, one G-Link©-200 wireless accelerometer with the sampling frequency of 512 Hz is placed on the car, as seen in Fig. 5.

As a verification, the acceleration data are collected from the bridge using three G-Link©-200 wireless accelerometers with the sampling frequency of 512 Hz. In order to detect as many modes as possible, these sensors are mounted at mid-span, quarter-span, and 3/8th-span of both bridges, shown previously in Fig. 1, which guarantees capturing the vibration of at least first four modes, based on the approximate mode shapes of the pin-roller and fixed-fixed beams.

Analysis

In this section, the analysis results are discussed in three parts. First, modal analysis of the bridge is conducted through free and tapping-forced vibration tests. Then, frequency content of the vibration of the car is investigated through non-moving suspension tests and moving off-bridge tests. Finally, moving car over the bridge is investigated.

Frequency analysis of the bridge

This section provides an overview of the natural frequencies of two bridges considered in this study. First, a free vibration test is performed on each bridge by applying an initial deflection at 40% span length. Applying initial deflection to this point not only creates relatively larger amplitude vibration, but also excites at least the first four modes of both bridges. Fig. 7 illustrates the ADFT spectrum of the acceleration signals. The three columns in this figure represent three sensors located on the bridge, and two rows represent two considered bridges. The fundamental frequency of the pin-roller and fixed-fixed bridges are identified as 7.6 and 9 Hz, respectively. As expected, the amplitudes of the 1st and 3rd modes are significant in the mid-span sensor spectrum, while 2nd and 4th have a relatively major presence in the quarter-span sensor spectrum, especially in the fixed-fixed bridge. The other observation is that the first mode always has the largest amplitude in the free vibration test.

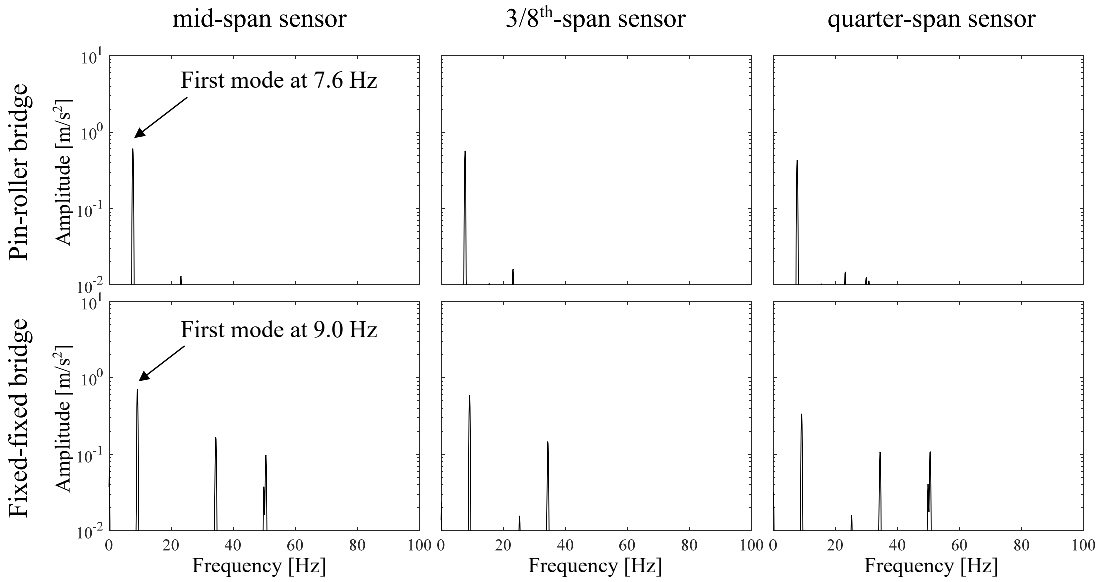

Fig. 7. ADFT Spectrum of bridge sensors under free vibration of the bridge

In order to identify higher mode frequencies with higher accuracy and larger amplitudes, another test was conducted through multiple tapping over different points along the bridge, to mimic ambient vibration tests. This way, higher modes of the bridge are excited and higher peaks appear due to those modes, as seen in Fig. 8, which has a similar organization to Fig. 7. Considering the frequency range of 0~100 Hz, 2nd and 3rd modes of the pin-roller bridge are 29.9 and 65.7 Hz, and 2nd to 5th modes of the fixed-fixed bridge are 26, 34.1, 50.3, and 69.8 Hz, respectively.

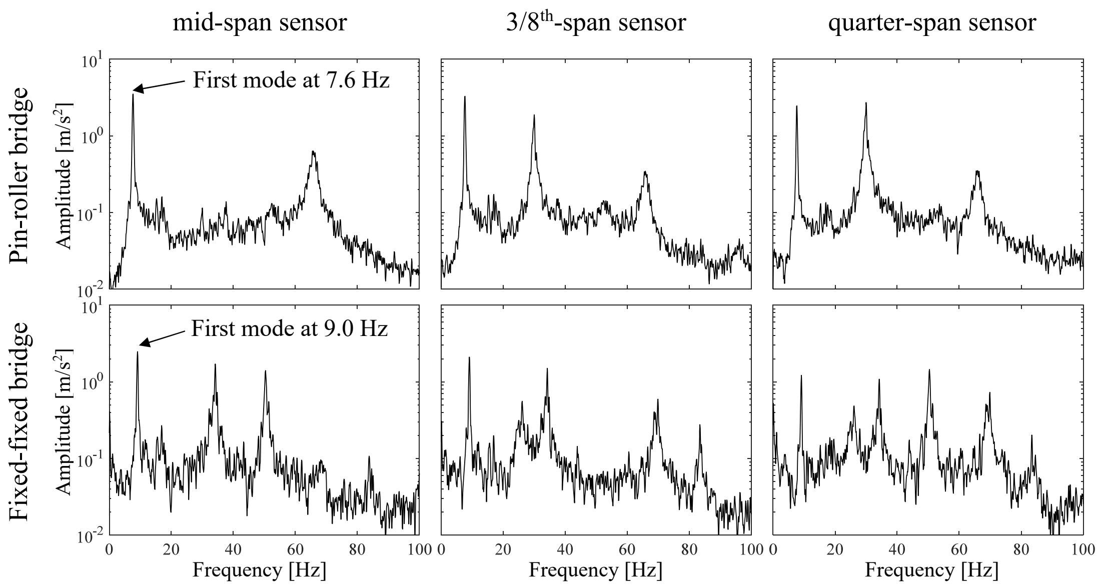

Fig. 8. ADFT Spectrum of bridge sensors under tapping-forced vibration of the bridge

Frequency analysis of the robot car

The aim of this section is to experimentally investigate the frequency content of the vibration of the robot car considering three different suspension systems. First, the suspension system of the car is studied through a free vibration test, which is performed by applying an initial deflection to the top plate of the car when the car is at a stationary position. Since the damping of the suspension system in this model is very large due to imperfections, the length of the free vibration signal is very short, i.e. around two seconds. Thus, the ADFT analysis was conducted using smaller windows, resulting in a very smooth spectrum in Fig. 9. This figure has three rows representing three spring types used in this study, and each graph contains two curves related to the sensor and the smartphone mounted on the car. As seen, the frequency of the suspension system is clearly visible in all three graphs and is equal to 3.9, 5, and 5.4 Hz, for three springs of A, B, and C, respectively. As expected, the frequency of the suspension system increases with the stiffness of the springs.

Another important observation in this figure is that the spectrum of the sensor and the smartphone agree in capturing the peak, but with different amplitudes. Since the main focus of this study is to find the significant frequencies in the spectrum, it means that smartphones can be considered a reliable tool for this purpose.

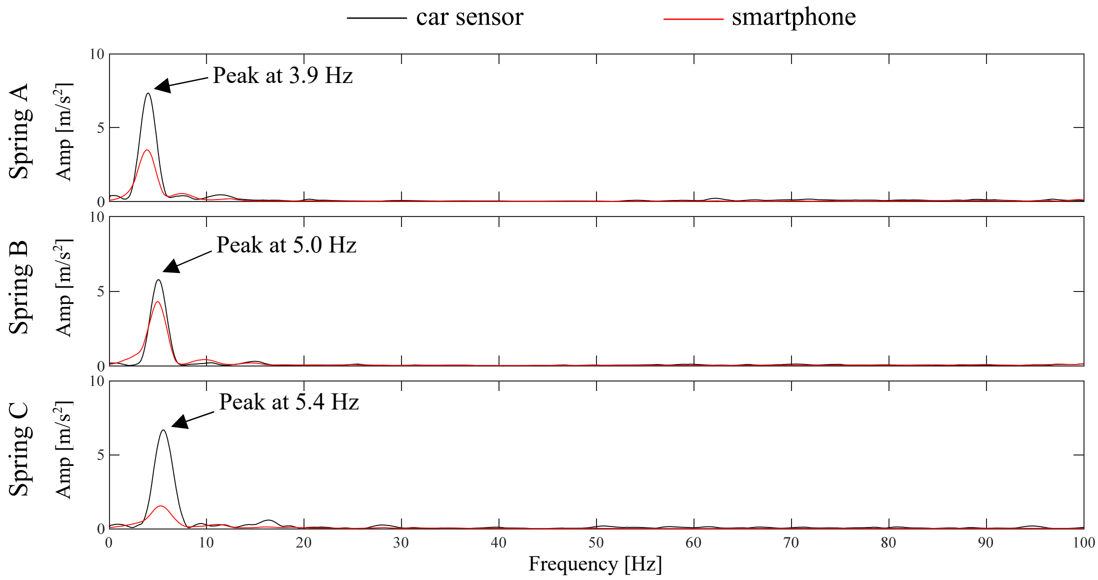

Fig. 9. ADFT Spectrum of the car sensor and smartphone under suspension test using three different springs

After analyzing the suspension system, the vibration analysis of the car while moving on a rigid surface, i.e. off-bridge test, is conducted. Such a test could be suitable for comparing the vibration of the same car moving on the bridge, in order to investigate the effect of the bridge on the car vibration. Fig. 10 demonstrates the spectrum of the sensor and the smartphone mounted on the car in different conditions. Three columns in this figure illustrate the speed values of the car, while three rows represent different springs and hence different suspension systems. As seen, there are three major peak ranges visible in these graphs. Considering v=0.2 m/s, there are multiple peaks at around 14, 30, and 54 Hz. However, these peaks change to 18.5, 34, and 67.5 in v=0.3 m/s, and 22, 43, and 85 in v=0.4 m/s, respectively. On the other hand, the columns of Fig. 10 prove that these peaks do not change with suspension system of the car. In fact, based on the results from Fig. 9, the frequencies of the suspension system are all below 10 Hz, which are not significantly excited in this experiment in Fig. 10. The reason could be the fact that unless there is a huge surface disruption, like potholes, the suspension frequency will be noticeably less excited with respect to other sources of vibration, like motor vibration or the moving frequency of the vehicle. In addition, similar to Fig. 9, this experiment corroborates the application of smartphones to detect frequency content of the car.

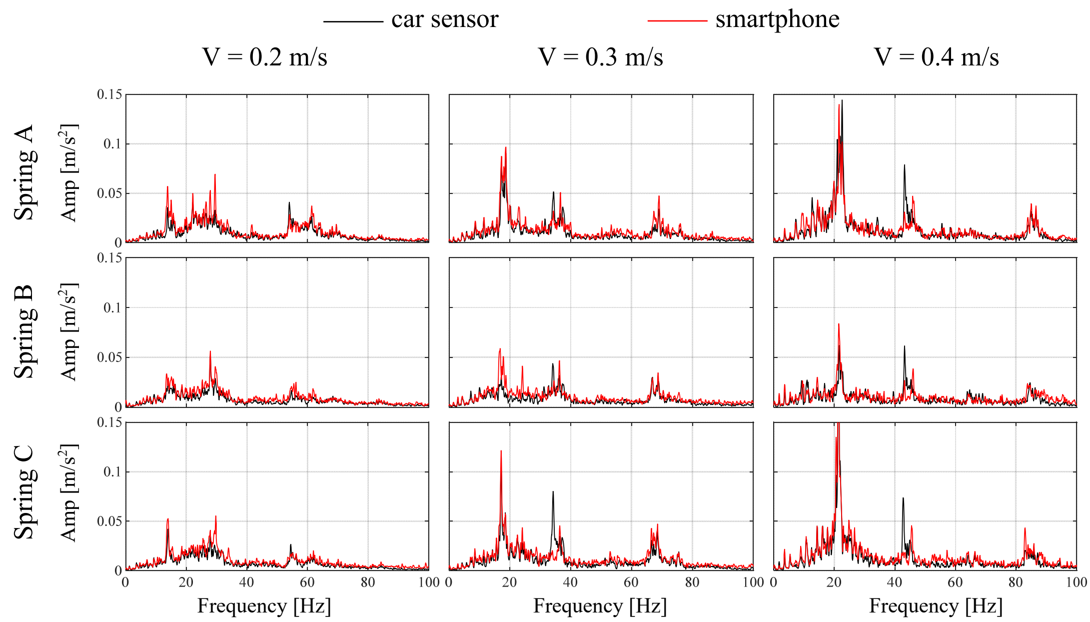

Fig. 10. ADFT Spectrum of the car sensor and smartphone under off-bridge test using three different springs at three different speeds

Frequency analysis of the robot car moving on the bridge

In this section, the vibration recorded on the car while moving on the bridge is studied. Similar to the previous section of Frequency analysis of the bridge, first the condition of the moving car as the only source of vibration, i.e. with no external force acting on the bridge, is considered. Afterward, along with the car moving, multiple tapping on different points on the bridge is applied, to account for larger vibrations of the bridge due to other forces, such as other cars or wind loads. Comparing the frequency contents of this section with those of off-bridge experiment in the previous section of Frequency analysis of the robot car makes it possible to identify the effect of bridge vibration on the recorded acceleration on the car.

Fig. 11 and Fig. 12 show the spectrums of the car moving over pin-roller and fixed-fixed bridges, respectively, while there are no external forces acting on the bridge. The organizations of both figures are similar to Fig. 10 except that there are vertical dashed lines added to the graphs showing the first three frequencies of each bridge identified through the bridge experiments. Both Fig. 11 and Fig. 12 almost show the same pattern seen in the off-bridge analysis, Fig. 10, with the only difference that there is one extra relatively sharp peak below 10 Hz, close to the fundamental frequency of the bridge. In Fig. 11, the first peak in the first column, i.e. when $v=0.2m/s$, is equal to 7.3 Hz, while this peak changes to 7.2 and 7 Hz for $v=0.3m/s$ and $v=0.4m/s$, respectively. This deviation from the exact bridge frequency, 7.6 Hz, verifies the previously shown phenomena of shifted frequency (Yang et al. 2004) of the bridge in the vibration of the car, which increases with the speed of the vehicle. Likewise, in Fig. 12, the identified frequencies of the bridge are 8.7, 8.6, and 8.4 for $v=0.2m/s$, $v=0.3m/s$, and $v=0.4m/s$, respectively, compared to the exact fundamental frequency of 9 Hz.

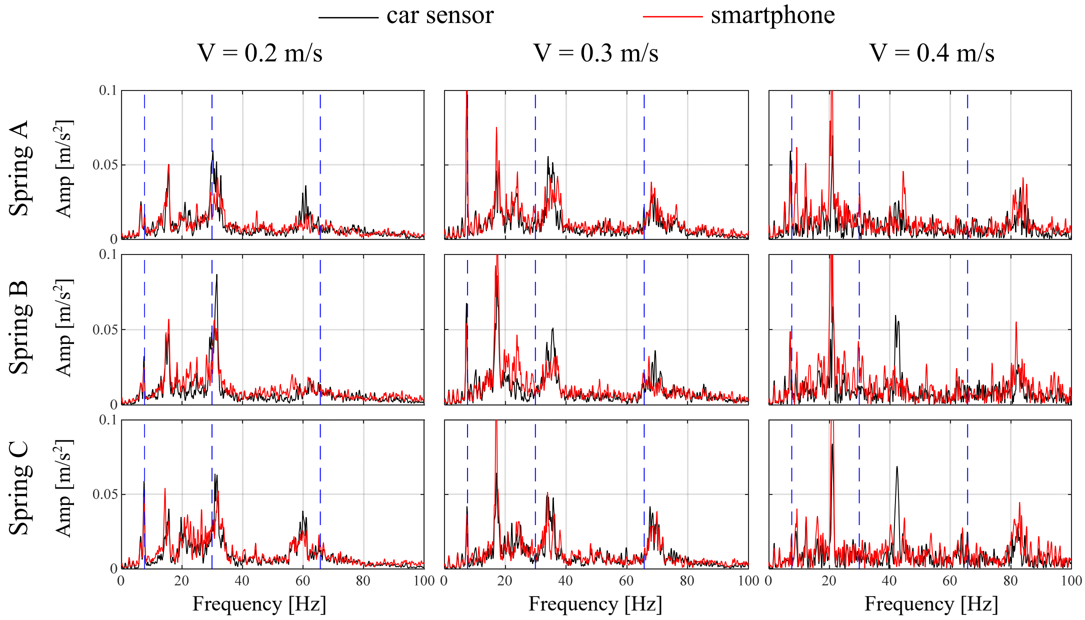

Fig. 11. ADFT Spectrum of the car sensor and smartphone under free on-bridge test on the pin-roller bridge using three different springs at three different speeds

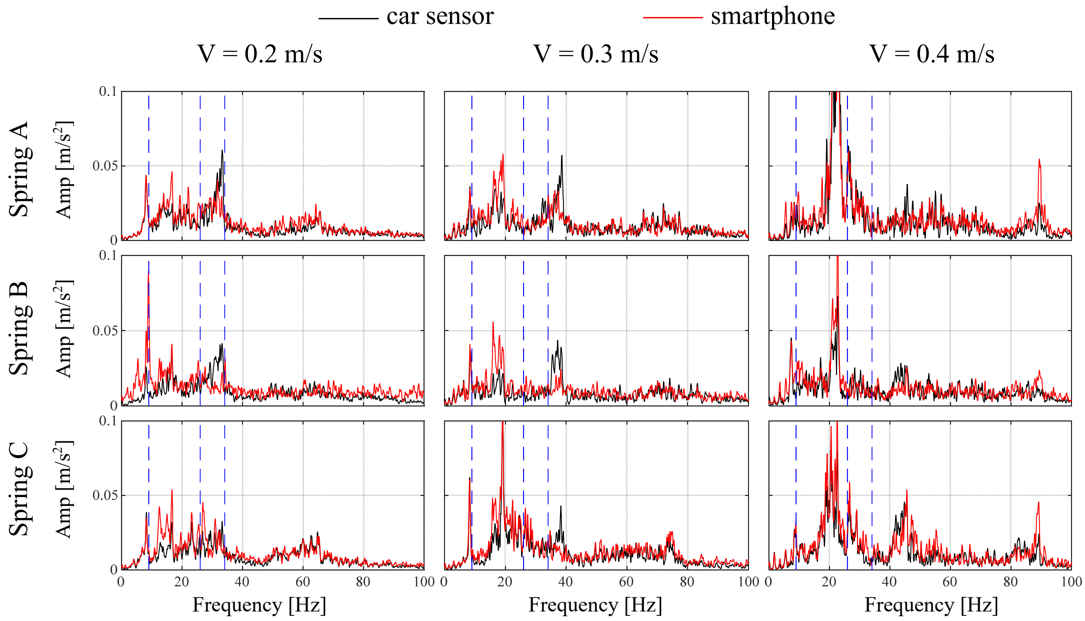

Fig. 12. ADFT Spectrum of the car sensor and smartphone under free on-bridge test on the fixed-fixed bridge using three different springs at three different speeds

As seen in both Fig. 11 and Fig. 12, it seems that higher modes are either not excited or their amplitude is very low when there is no other source of excitation except the moving car. In fact, in this experiment, the higher modes of the bridge, excited with relatively lower amplitudes, lie within the peaks of the car spectrum, excited with significantly larger amplitudes, preventing those modes to be visible in the combined vibration spectrum.

However, the fundamental frequency of the bridge is below 10 Hz, where there are no significant peaks visible in the off-bridge spectrum in Fig. 10.

In real life situations, there are many sources of excitation acting simultaneously on the bridge, e.g. many cars moving in multiple lanes in similar or opposite directions, effects of winds, etc., which results in larger vibration of the bridge and hence stronger presence of its frequencies in the car spectrum. Therefore, another set of experiments was conducted by tapping multiple points along the bridge while the car moves over the bridge. Fig. 13 and Fig. 14 illustrate the spectrum of the car vibration during this experiment for pin-roller and fixed-fixed bridges, respectively. As expected, the presence of tapping-forced excitation that mimics other real-life sources of excitation increases the bridge vibration, resulting in a clear significant peak close to the fundamental frequency of the bridge. In addition, in some cases for pin-roller bridge and nearly all cases in the fixed-fixed bridge, the second mode of the bridge is also clearly present in the car spectrum.

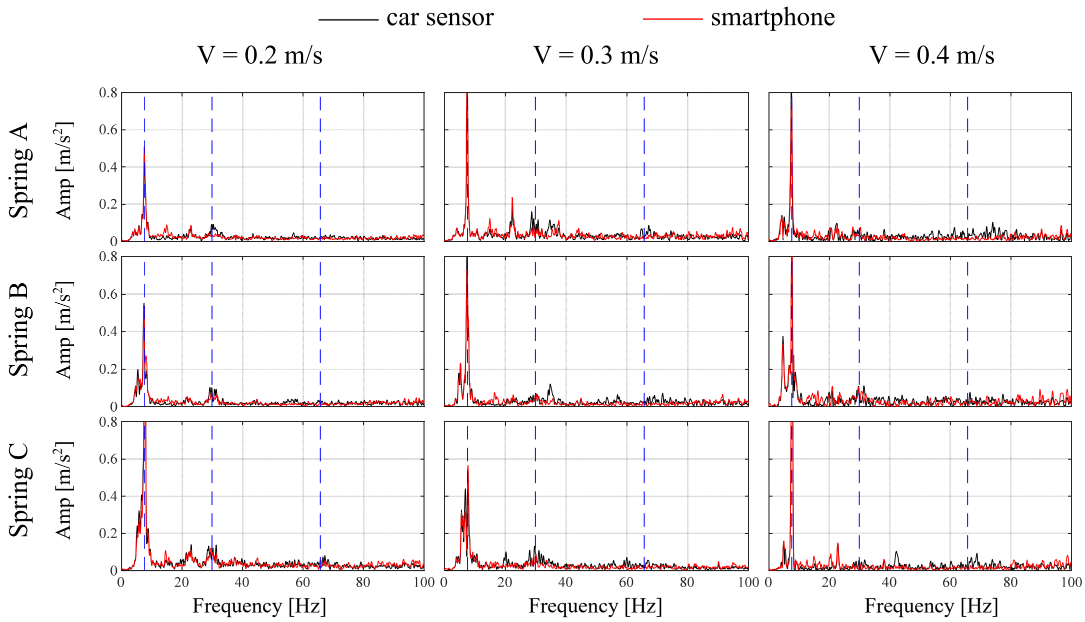

Fig. 13. ADFT Spectrum of the car sensor (black line) and smartphone (red line) under tapping-forced on-bridge test on the pin-roller bridge using three different springs at three different speeds

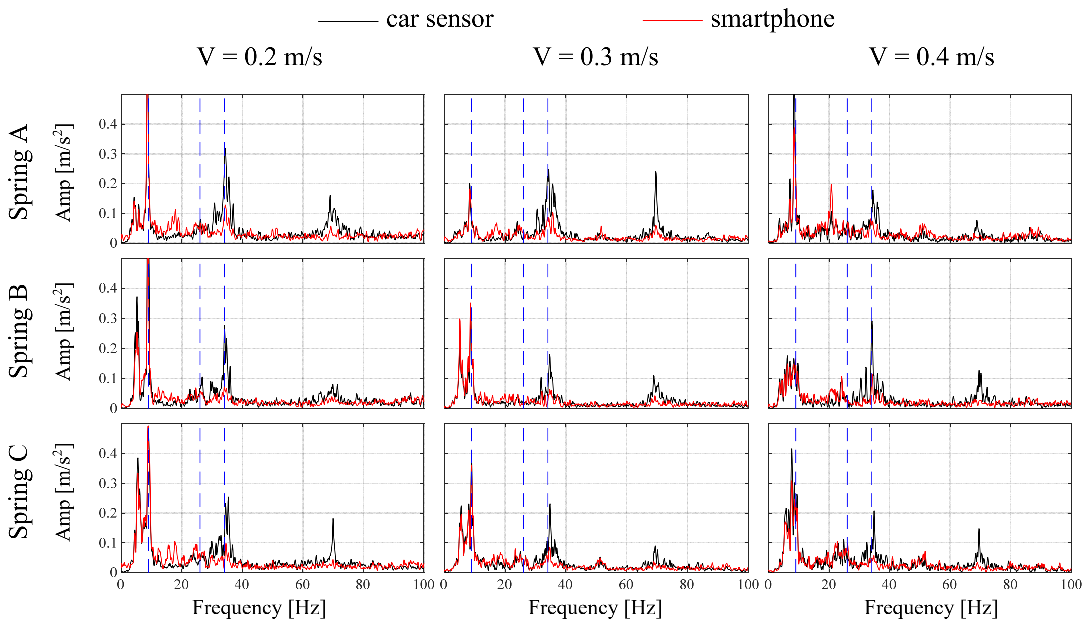

Fig. 14. ADFT Spectrum of the car sensor and smartphone under tapping-forced on-bridge test on the fixed-fixed bridge using three different springs at three different speeds

The important conclusion from this section is that if there is a substantial difference between the frequencies of the bridge and different cars passing over the bridge, it is possible to detect the shifted fundamental frequency of the bridge using the acceleration signal of the car recorded on the smartphone. In addition, with sufficient vibration of the bridge, there is a potential that second mode of the bridge could be captured as well. Moreover, it should be noted that, in future studies, the speed of the car while crossing the bridge can be easily obtained using the built-in GPS of smartphone and this information can be used to eliminate the effects of the speed on the identified frequencies.

Application to Bridge State Detection

This section focuses on the application of the proposed frequency analysis of smartphone data for assessing the changes in the structural condition of the bridge. Consider a large number of smartphones, as sources of data, located on many cars with different systems traveling over a bridge at different speeds. It is shown in this paper that it is possible to capture at least the first shifted frequency of the bridge through frequency analysis of the acceleration signals recorded on smartphones. At this point, the main challenge is the damage detection capability of such signals.

In order to investigate the potential of the framework presented in this paper for damage detection of bridges, analysis results presented in the previous sections are compared in Fig. 15**Error! Reference source not found.**. The organization of this figure is similar to previous figures containing all cases of different suspension systems at different speeds. However, each graph contains three curves: off-bridge spectrum with a black solid line, on-bridge spectrum over the pin-roller bridge with a red solid line, and on-bridge spectrum over the fixed-fixed bridge with a blue solid line, all using recorded signals with the smartphone. In addition, exact values of the fundamental frequencies of both bridges are shown using dashed lines, i.e. red line for pin-pin bridge and blue line for fixed-fixed bridge. Note that a narrow range of 0~20 Hz has been selected to concentrate on the fundamental frequency of the bridge in the spectrums.

Fig. 15**Error! Reference source not found.** illustrates that if there are many different vehicles moving over a bridge, it is possible to identify changes in the frequency of the bridge in most cases, although this deviation is not clearly captured in some cases, especially in higher speeds. The off-bridge spectrum provides a reliable tool to distinguish between car-related and bridge related peaks. Although the source and amount of the shift in the frequency of the bridge is still unknown and a subject of contention in the literature, these experiments demonstrate that it is possible to use smartphone data to detect changes in the bridge state, such as boundary conditions. The relatively large mass ratio of the robot car to the bridge in the experiments plays a major role in increasing the shift of the identified frequency since the mass distribution of the system changes as the car passes over the bridge and the frequency tends to be smaller due to larger total weight. It is expected that in real-life practice with lower mass ratio of car to bridge, the amount of the shift would be smaller.

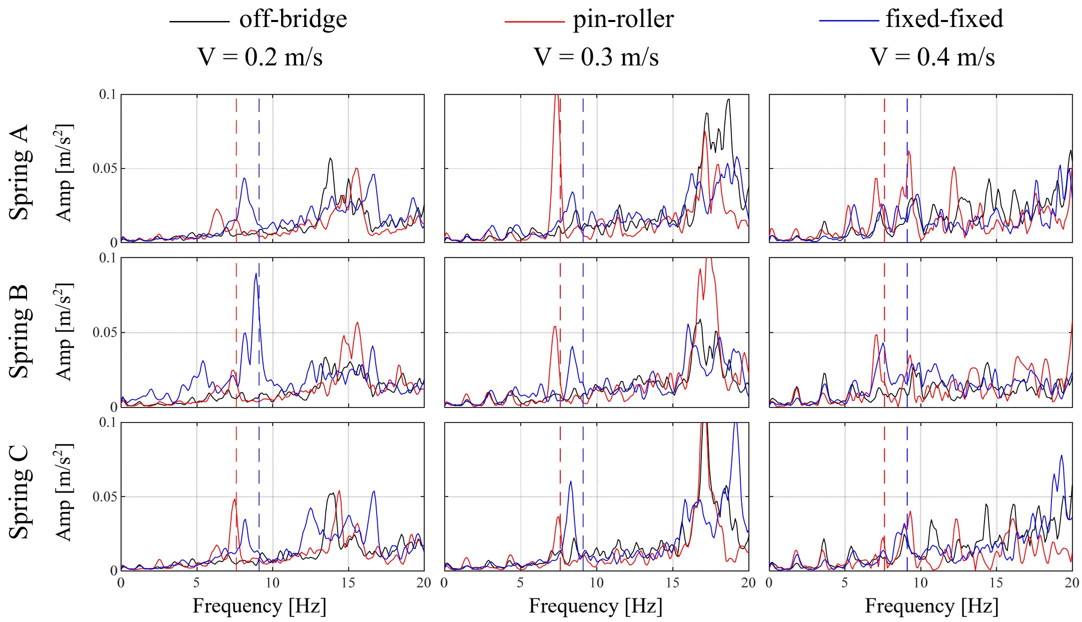

Fig. 15. ADFT Spectrum of the smartphone under off-bridge test, on-bridge test over the pin-roller bridge, and on-bridge test over the fixed-fixed bridge using three different springs at three different speeds

In order to investigate the capability of detecting bridge frequency, the peak picking technique described in the Methodology section is employed to the data in Fig. 15. The resulting peak scores are then used to find the most probable range for the frequency of both pin-pin and fixed-fixed bridges. For this purpose, successive 0.5 Hz-wide windows are considered in each spectrum and the score of all peaks in those windows are averaged. This averaged score represents the significance of the peaks in each frequency range of that spectrum. Comparing averaged peak scores for each frequency range among two different passes, i.e. off-bridge, pin-pin, or fixed-fixed bridge, makes it possible to detect the frequency range with the largest score change, which represents the frequency range of the corresponding bridge.

This process is conducted on all different combinations of suspension and speed shown in Fig. 15 and the results are illustrated in Figs. 16-18. The red and blue dashed lines in these figures show the fundamental frequency of pin-pin and fixed-fixed bridges, respectively. Fig. 16 demonstrates the change in the averaged peak score of pin-pin bridge with respect to off-bridge condition. As seen, the largest increase in the averaged peak score is in 7-8 Hz range, which are close to the exact frequency of 7.6 Hz. It is expected that most of the bridge-related peaks are smaller than 7.6 since the shifted frequency is expected to be smaller. Similarly, Fig. 17 that represents the change in the averaged peak score of fixed-fixed bridge with respect to off-bridge shows the most changes in 7.5-9 Hz, close to 9 Hz of fixed-fixed bridge fundamental frequency.

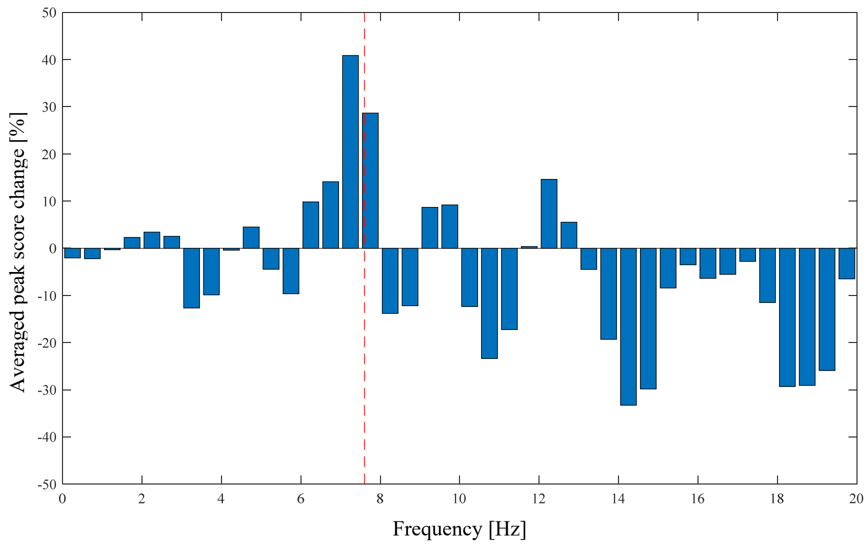

Fig. 16. Averaged peak score change of all passes on pin-pin bridge vs. off-bridge

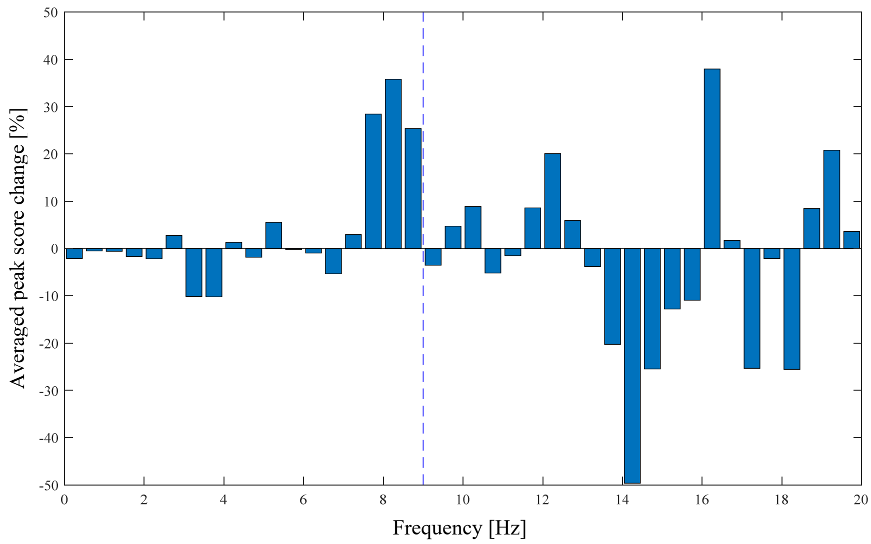

Fig. 17. Averaged peak score change of all passes on fixed-fixed bridge vs. off-bridge

More insights are provided by comparing the passes over pin-pin and fixed-fixed bridges. Fig. 18 illustrates the same score change described in Fig. 16 and Fig. 17 considering the fixed-fixed bridge as the baseline. As seen, there is a large drop in the averaged peak score of the frequencies near fixed-fixed bridge, while there is a large increase close to that of the pin-pin bridge. This plot represents the main output of this section, which is bridge state detection. Using the vibration data from different cars with different speeds passing over two different bridge states, this methodology would be able detect the change in the frequency of those bridges without a prior knowledge of their frequency.

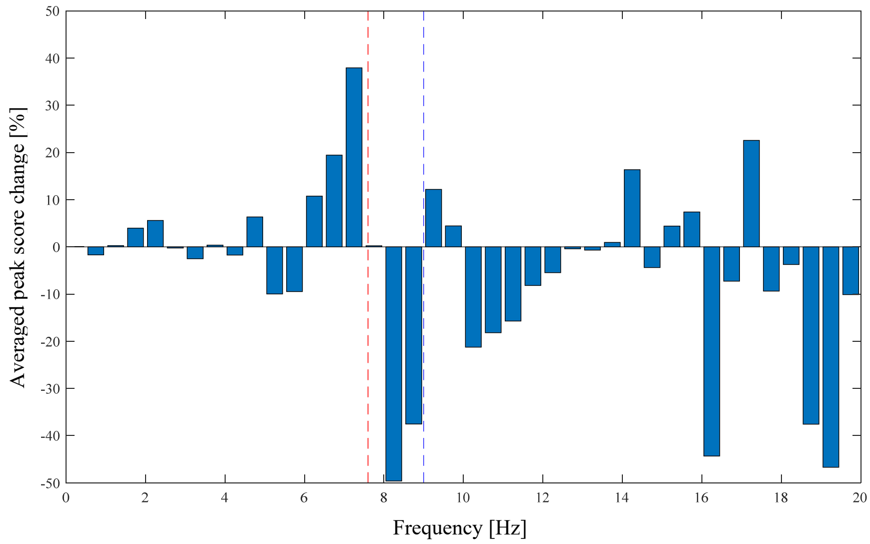

Fig. 18. Averaged peak score change of all passes on pin-pin bridge vs. fixed-fixed bridge

It is noteworthy that the resolution and accuracy of the identified frequencies are expected to increase with the use of future smartphones as the quality and performance of the built-in sensors in smartphones increase considerably in time. For example, the maximum sampling frequency for a Samsung Galaxy S5 is 200Hz whereas it is 400Hz for the Samsung Galaxy s8 used for the experiments presented in this paper. Such developments in technology will further increase the benefits of the framework presented in this paper.

Conclusions

This study proposes a crowdsensing framework for utilizing smartphone data to evaluate populations of bridges in future smart cities. The analysis framework and experimental results presented in this paper demonstrate that the fundamental frequency and possibly higher mode frequencies of a bridge can be detected by analyzing the vibration data recorded using a smartphone on a vehicle crossing the bridge. Different combinations of the suspension springs and speeds for the vehicle as well as considering two bridges with different support systems provide strong evidence for the robustness of the method against vehicle and bridge properties. In addition, since any severe damage to the bridge will have a significant impact on its fundamental frequency, this study proves that there is a possibility that such damage could be identified through an appropriate crowdsensing framework which gathers data from a large population of smartphones on different cars passing over a bridge. Furthermore, this study shows that despite the fact that the identified frequency of the bridge using vibration data of the vehicle is shifted, and the magnitude of this shift is still unknown for different vehicle-bridge systems, it is still possible to successfully detect the frequency change of the bridge. It is noted that the surface roughness is expected to play a significant role in the recorded acceleration signals and its effect on the performance of the proposed methodology needs to be investigated in future studies. The most significant factor on the frequency shift was identified as the speed of the car, which can be recorded through GPS sensor inside the smartphone without the need of installing extra sensors.

Acknowledgments

The financial support from the corresponding author's NSERC Discovery Grant is gratefully acknowledged.

References

Adeli, H., and Jiang, X. (2009). *Intelligent infrastructure. Neural networks, wavelets, and chaos theory for intelligent transportation systems and smart structures*. CRC press.

Bhoraskar, R., Vankadhara, N., Raman, B., and Kulkarni, P. (2012). "Wolverine: Traffic and road condition estimation using smartphone sensors." *4th International Conference on Communication Systems and Networks, COMSNETS 2012*, IEEE, 1–6.

Canadian Infrastructural Report Card. (2016*). Informing the future: assessing the health of our communities' infrastructure.*

Catbas, F. N., Gul, M., and Burkett, J. L. (2008). "Conceptual damage-sensitive features for structural health monitoring: Laboratory and field demonstrations." *Mechanical Systems and Signal Processing*, 22(7), 1650–1669.

Cerda, F., Chen, S., Bielak, J., Garrett, J. H., Rizzo, P., and KovaČević, J. (2014). "Indirect structural health monitoring of a simplified laboratory-scale bridge model." *Smart Structures and Systems*, 13(5), 849–868.

Chourabi, H., Nam, T., Walker, S., Gil-Garcia, J. R., Mellouli, S., Nahon, K., Pardo, T. A., and Scholl, H. J. (2012). "Understanding smart cities: An integrative framework." *Proceedings of the Annual Hawaii International Conference on System Sciences*, IEEE, 2289–2297.

Feng, M., Fukuda, Y., Mizuta, M., and Ozer, E. (2015). "Citizen sensors for SHM: Use of accelerometer data from smartphones." *Sensors (Switzerland)*, MDPI AG, 15(2), 2980–2998.

Glancy, D. J. (2014). "Sharing the road: Smart transportation infrastructure." *Fordham Urb*. LJ, XLI, 1617–1664.

Graham, S. (2010). *Disrupted cities : when infrastructure fails*. University of Waterloo. Routledge.

Guan, S., Bridge, J. A., Li, C., and DeMello, N. J. (2018). "Smart radar sensor network for bridge displacement monitoring." *Journal of Bridge Engineering*, 24(1), 04018102.

Gul, M., and Catbas, F. N. (2009). "Statistical pattern recognition for Structural Health Monitoring using time series modeling: Theory and experimental verifications." *Mechanical Systems and Signal Processing*, Elsevier, 23(7), 2192–2204.

Ham, H., Kim, T. J., and Boyce, D. (2005). "Assessment of economic impacts from unexpected events with an interregional commodity flow and multimodal transportation network model." *Transportation Research Part A: Policy and Practice*, 39(10), 849–860.

Händel, P., Ohlsson, J., Ohlsson, M., Skog, I., and Nygren, E. (2014). "Smartphone-based measurement systems for road vehicle traffic monitoring and usage-based insurance." *IEEE Systems Journal*, 8(4), 1238–1248.

Harris, F. J. (1978). "On the use of windows for harmonic analysis with the discrete Fourier transform." *Proceedings of the IEEE*, 66(1), 51–83.

Hattori, H., He, X., Catbas, F. N., Furuta, H., and Kawatani, M. (2012). "A bridge damage detection approach using vehicle-bridge interaction analysis and neural network technique." *Bridge Maintenance, Safety, Management, Resilience and Sustainability*, 376-383.

Hester, D., and González, A. (2017). "A discussion on the merits and limitations of using drive-by monitoring to detect localised damage in a bridge." *Mechanical Systems and Signal Processing*, Academic Press, 90, 234–253.

Hoult, N. A., Fidler, P. R. A., Hill, P. G., and Middleton, C. R. (2010). "Long-term wireless structural health monitoring of the ferriby road bridge." *Journal of Bridge Engineering*, 15(2), 153–159.

Hsieh, K. H., Halling, M. W., and Barr, P. J. (2006). "Overview of vibrational structural health monitoring with representative case studies." *Journal of Bridge Engineering*, 11(6), 707–715.

Keenahan, J., OBrien, E. J., McGetrick, P. J., and Gonzalez, A. (2014). "The use of a dynamic truck-trailer drive-by system to monitor bridge damping." *Structural Health Monitoring*, 13(2), 143–157.

Kim, C., Isemoto, R., Toshinami, T., Kawatani, M., McGetrick, P., O'Brien, E. J. (2011). "Experimental investigation of drive-by bridge inspection." *5th International Conference* *on Structural Health Monitoring of Intelligent Infrastructure (SHMII-5)*. Cancun, Mexico: Instituto de Ingeniería, UNAM.

Kim, J., and Lynch, J. P. (2012). "Experimental analysis of vehicle-bridge interaction using a wireless monitoring system and a two-stage system identification technique." *Mechanical Systems and Signal Processing*, Elsevier, 28, 3–19.

Ko, J. M., and Ni, Y. Q. (2005). "Technology developments in structural health monitoring of large-scale bridges." *Engineering structures*, Elsevier, 27(12), 1715–1725.

Kong, Q., Allen, R. M., Kohler, M. D., Heaton, T. H., and Bunn, J. (2018). "Structural health monitoring of buildings using smartphone sensors." *Seismological Research Letters*, Seismological Society of America, 89(2A), 594–602.

Li, J., Zhu, X., Law, S., and Samali, B. (2019). "Drive-by blind modal identification with singular spectrum analysis." *Journal of Aerospace Engineering*, 32(4): 04019050.

Lin, C. W., and Yang, Y. B. (2005). "Use of a passing vehicle to scan the fundamental bridge frequencies: An experimental verification." *Engineering Structures*, 27(13), 1865–1878.

Malekjafarian, A., McGetrick, P. J., and Obrien, E. J. (2015). "A review of indirect bridge monitoring using passing vehicles." *Shock and Vibration*, Hindawi Limited.

Matarazzo, T. J., Santi, P., Pakzad, S. N., Carter, K., Ratti, C., Moaveni, B., Osgood, C., and Jacob, N. (2018). "Crowdsensing framework for monitoring bridge vibrations using moving smartphones." *Proceedings of the IEEE*, 106(4), 577–593.

Mathworks. (2018). "MATLAB, the language of technical computing."

Mei, Q., and Gül, M. (2018). "A crowdsourcing-based methodology using smartphones for bridge health monitoring." *Structural Health Monitoring*. DOI: 10.1177/1475921718815457.

Mei, Q., Gül, M., and Boay, M. (2019). "Indirect health monitoring of bridges using Mel-frequency cepstral coefficients and principal component analysis." *Mechanical Systems and Signal Processing*, Elsevier Ltd, 119, 523–546.

Mohan, P., Padmanabhan, V. N., and Ramjee, R. (2008). "Nericell: Rich monitoring of road and traffic conditions using mobile smartphones." *Proceedings of the 6th ACM conference on Embedded network sensor systems*, 323–336.

Morgenthal, G., Rau, S., Taraben, J., and Abbas, T. (2018). "Determination of stay-cable forces using highly mobile vibration measurement devices." *Journal of Bridge Engineering*, 23(2), 04017136.

OBrien, E. J., Malekjafarian, A., and González, A. (2017). "Application of empirical mode decomposition to drive-by bridge damage detection." *European Journal of Mechanics*, A/Solids, Elsevier Ltd, 61, 151–163.

Ozer, E., and Feng, M. Q. (2016). "Synthesizing spatiotemporally sparse smartphone sensor data for bridge modal identification." *Smart Materials and Structures*, Institute of Physics Publishing, 25(8).

Ozer, E., and Feng, M. Q. (2017). "Direction-sensitive smart monitoring of structures using heterogeneous smartphone sensor data and coordinate system transformation." *Smart Materials and Structures*, Institute of Physics Publishing, 26(4).

Siringoringo, D. M., and Fujino, Y. (2012). "Estimating bridge fundamental frequency from vibration response of instrumented passing vehicle: Analytical and experimental study." *Advances in Structural Engineering*, 15(3), 417–433.

Washburn, D., Sindhu, U., Balaouras, S., Dines, R., Hayes, N., and Nelson, L. (2010). "Helping CIOs understand 'Smart City' initiatives." *Forrester Research Inc.*, 17.

Welch, P. D. (1967). "The use of fast Fourier transform for the estimation of power spectra: A method based on time averaging over short, modified periodograms." *IEEE Transactions on Audio and Electroacoustics*, 15(2), 70–73.

Wenzel, H. (2008). *Health monitoring of bridges*. John Wiley & Sons.

Wong, K.-Y. (2004). "Instrumentation and health monitoring of cable-supported bridges." *Structural Control and Health Monitoring*, 11(2), 91–124.

Xiong, Z., Sheng, H., Rong, W. G., and Cooper, D. E. (2012). "Intelligent transportation systems for smart cities: A progress review." *Science China Information Sciences*, 55(12), 2908–2914.

Yang, Y. B., and Chen, W. F. (2016). "Extraction of bridge frequencies from a moving test vehicle by stochastic subspace identification." *Journal of Bridge Engineering*, 21(3), 04015053.

Yang, Y. B., Lin, C. W., and Yau, J. D. (2004). "Extracting bridge frequencies from the dynamic response of a passing vehicle." *Journal of Sound and Vibration*, 272(3–5), 471–493.

Zhang, Y., Lie, S. T., and Xiang, Z. (2013). "Damage detection method based on operating deflection shape curvature extracted from dynamic response of a passing vehicle." *Mechanical Systems and Signal Processing*, Elsevier, 35(1–2), 238–254.

Zhao, X., Han, R., Yu, Y., Hu, W., Jiao, D., Mao, X., Li, M., and Ou, J. (2017). "Smartphone-based mobile testing technique for quick bridge cable-force measurement." *Journal of Bridge Engineering*, 22(4), 06016012.

Figure Caption List

Fig. 1. Pin-roller bridge setup

Fig. 2. Pin/roller support

Fig. 3. Fixed-fixed bridge setup

Fig. 4. Fixed support

Fig. 5. The custom-designed and -built robot car

Fig. 6. Robot car on the fixed-fixed bridge

Fig. 7. ADFT Spectrum of bridge sensors under free vibration of the bridge

Fig. 8. ADFT Spectrum of bridge sensors under tapping-forced vibration of the bridge

Fig. 9. ADFT Spectrum of the car sensor and smartphone under suspension test using three different springs

Fig. 10. ADFT Spectrum of the car sensor and smartphone under off-bridge test using three different springs at three different speeds

Fig. 11. ADFT Spectrum of the car sensor and smartphone under free on-bridge test on the pin-roller bridge using three different springs at three different speeds

Fig. 12. ADFT Spectrum of the car sensor and smartphone under free on-bridge test on the fixed-fixed bridge using three different springs at three different speeds

Fig. 13. ADFT Spectrum of the car sensor (black line) and smartphone (red line) under tapping-forced on-bridge test on the pin-roller bridge using three different springs at three different speeds

Fig. 14. ADFT Spectrum of the car sensor and smartphone under tapping-forced on-bridge test on the fixed-fixed bridge using three different springs at three different speeds

Fig. 15. ADFT Spectrum of the smartphone under off-bridge test, on-bridge test over the pin-roller bridge, and on-bridge test over the fixed-fixed bridge using three different springs at three different speeds

Fig. 16. Averaged peak score change of all passes on pin-pin bridge vs. off-bridge

Fig. 17. Averaged peak score change of all passes on fixed-fixed bridge vs. off-bridge

Fig. 18. Averaged peak score change of all passes on pin-pin bridge vs. fixed-fixed bridge